CAMBRIDGE
UNIVERSITY PRESS

Article

Alumolukrahnite, CaCu²⁺Al(AsO₄)₂(OH)(H₂O), the aluminium analogue of lukrahnite from the Jote mine, Copiapó Province, Chile

Anthony R. Kampf[1]* , Stuart J. Mills[2], Barbara P. Nash[3], Maurizio Dini[4] and Arturo A. Molina Donoso[5]

[1]Mineral Sciences Department, Natural History Museum of Los Angeles County, 900 Exposition Boulevard, Los Angeles, CA 90007, USA; [2]Geosciences, Museums Victoria, GPO Box 666, Melbourne 3001, Australia; [3]Department of Geology and Geophysics, University of Utah, Salt Lake City, Utah 84112, USA; [4]Central University of Chile, La Serena, Chile; and [5]Chilean Minerals, Iquique, Chile

Abstract

The new mineral alumolukrahnite (IMA2022–059), $CaCu^{2+}Al(AsO_4)_2(OH)(H_2O)$, was found at the Jote mine, Copiapó Province, Chile, where it is a secondary alteration phase associated with conichalcite, coronadite, gypsum, olivenite, pharmacosiderite, rruffite and scorodite. Alumolukrahnite occurs as crude diamond-shaped tablets up to ∼0.1 mm, intergrown in crude spherical aggregates. Crystals are apple green and transparent to translucent, with vitreous lustre and a white streak. The Mohs hardness is 3½. The mineral is brittle with irregular fracture and no cleavage. The calculated density is 4.094 g cm⁻³. Optically, alumolukrahnite is biaxial (+) with $\alpha = 1.73(1)$, $\beta = 1.74(1)$ and $\gamma = 1.76(1)$ (white light). The empirical formula, determined from electron microprobe analyses, is $Ca_{1.01}(Cu_{0.92}Zn_{0.13})_{\Sigma1.05}(Al_{0.96}Fe_{0.01})_{\Sigma0.97}(As_{0.985}O_4)_2(OH)_{0.88}(H_2O)_{1.12}$. Alumolukrahnite is triclinic, $P\bar{1}$, $a = 5.343(5)$, $b = 5.501(5)$, $c = 7.329(5)$ Å, $\alpha = 67.72(2)$, $\beta = 69.06(2)$, $\gamma = 69.42(2)°$, $V = 180.3(3)$ Å³ and $Z = 1$. Alumolukrahnite is a member of the tsumcorite group and is the Al analogue of lukrahnite.

Introduction

The small mines and prospects of the Pampa Larga mining district in the Atacama Region of Chile have yielded a surprising variety of rare minerals, most of which contain essential arsenic. The four new minerals previously described from these deposits, alacránite, As_8S_9 (Popova *et al.*, 1986), rruffite, Ca_2Cu $(AsO_4)_2·2H_2O$ (Yang *et al.*, 2011), joteite, $Ca_2CuAl[AsO_4]$ $[AsO_3(OH)]_2(OH)_2·5H_2O$ (Kampf *et al.*, 2013) and tapiaite, $Ca_5Al_2(AsO_4)_4(OH)_4·12H_2O$ (Kampf *et al.*, 2015), all contain essential arsenic and three are arsenates. Joteite and tapiaite, both first described from the Jote mine, also contain both Ca and Al. There are numerous Ca-arsenate and Al-arsenate minerals; however, arsenates containing essential Ca and Al are very uncommon and include only eight mineral species. Described herein is the ninth Ca–Al arsenate, alumolukrahnite, also from the Jote mine.

The name alumolukrahnite reflects the fact that the mineral is the aluminium (alumo) analogue of lukrahnite, $CaCuFe^{3+}$ $(AsO_4)_2(OH)·H_2O$ (Krause *et al.*, 2001). The new mineral and the name (symbol Alkr) have been approved by the Commission on New Minerals, Nomenclature and Classification of the International Mineralogical Association. (IMA2022-059, Kampf *et al.*, 2023). The description is based upon three cotype

specimens deposited in the collections of the Natural History Museum of Los Angeles County, Los Angeles, California, USA, catalogue numbers 76256, 76257 and 76258.

Occurrence

The mineral occurs at the Jote mine, Pampa Larga district, Tierra Amarilla, Copiapó Province, Atacama Region, Chile. Mineralisation occurs in a narrow (20 to 40 cm wide) hydrothermal vein hosted by volcanoclastic rocks. The occurrence is similar to that of the mineral rruffite (Yang *et al.*, 2011) at the Maria Catalina mine in the same district. A detailed description of the geology and mineralogy of the area was provided by Parker *et al.* (1963). The specimens of alumolukrahnite were collected by one of the authors (AAMD) in 2011.

The deeper unoxidised portion of the vein contains primary and supergene minerals including acanthite, native arsenic, Ag sulfosalts, baryte, calcite, chalcopyrite, domeykite, feldspar, pyrite, quartz, native silver and stibnite. Alumolukrahnite occurs as a late-stage, low-temperature, secondary mineral in narrow seams and vughs in the oxidised upper portion of the vein. The matrix is an intergrowth of quartz and microcline–albite 'microperthite'. The microperthite varies from fresh to heavily altered. The more heavily altered areas are impregnated with massive mansfieldite and/or scorodite. Other secondary minerals in direct association with alumolukrahnite are conichalcite, coronadite, gypsum, olivenite, pharmacosiderite, rruffite and scorodite. Other minerals found in the oxidation zone include arseniosiderite, ceruleite, chlorargyrite, gartrellite, goudeyite, joteite, karibibite,

*Author for correspondence: Anthony R. Kampf, Email: akampf@nhm.org

koritnigite, krautite, lavendulan, metazeunerite, opal, tapiaite and zincolivenite

Physical and optical properties

Alumolukrahnite occurs as crude diamond-shaped tablets, to ~0.1 mm in maximum dimension, intergrown in crude spherical aggregates to ~0.5 mm in diameter (Figs 1 and 2). No twinning was observed. By analogy with gartrellite, tablets may be flattened on {111}; however, helmutwinklerite, another triclinic tsumcorite-group mineral, is tabular on {001} (Krause *et al.*, 1998). The Bravais–Friedel–Donnay–Harker principle (Donnay and Harker, 1937) predicts tablets flattened on {001} with the bounding forms {100} and {010}.

Crystals are transparent to translucent, with vitreous lustre and a white streak. The mineral does not fluoresce in long- or short-wave ultraviolet light. The Mohs hardness is 3½ based on scratch tests. The tenacity is brittle, fracture is irregular and no cleavage was observed. The density was not measured because Clerici solution of necessary purity was not available. The calculated density is 4.094 g·cm^{-3} for the empirical formula and 4.085 g·cm^{-3} for the ideal formula. The mineral is insoluble at room temperature in concentrated HCl or concentrated H_2SO_4.

Poor crystal quality made optical measurements very difficult. Even the smallest crystal fragments exhibited undulatory extinction. Alumolukrahnite is biaxial (+) with $\alpha = 1.73(1)$, $\beta = 1.74(1)$ and $\gamma = 1.76(1)$ (measured in white light). Poor crystal quality made conoscopic observation and extinction measurements impossible, so 2V could not be measured. The calculated 2V is 71°. Dispersion could not be observed and the optical orientation could not be determined. The mineral is non-pleochroic. The Gladstone–Dale compatibility $1 - (K_p/K_c)$ is 0.024 (excellent) for the empirical formula and 0.019 (superior) for the ideal formula (Mandarino, 2007).

Raman spectroscopy

Raman spectroscopy was done on a Horiba XploRa PLUS micro-Raman spectrometer using an incident wavelength of 532 nm, laser slit of 200 μm, 1800 gr/mm diffraction grating and a 100× (0.9 NA) objective. The spectrum recorded from 3800 to 60 cm^{-1} is shown in Fig. 3.
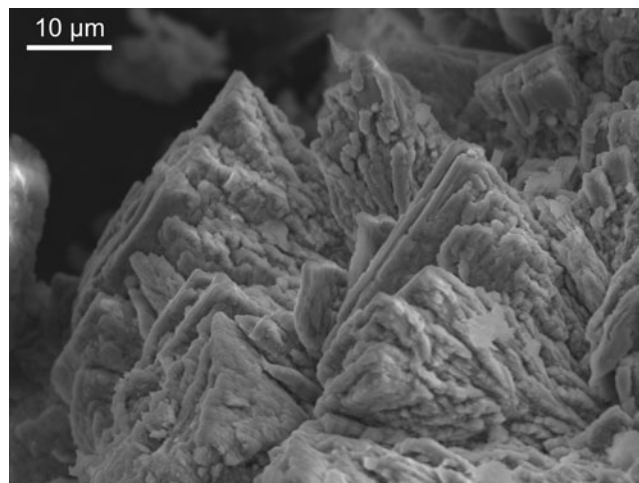

Fig. 2. Intergrowths of alumolukrahnite tablets (scanning electron microscopy image, specimen #76256).

The Raman spectrum exhibits general similarities to that reported by Frost *et al.* (2012) for gartrellite from the Ojuela mine, Durango, Mexico. The most important bands are related to the AsO_4 group. The bands at 884 and 850 can be assigned to ν_1 symmetric stretching vibrations and that at 819 cm^{-1} to ν_3 antisymmetric stretching. Those at 531 and 423 cm^{-1} relate to ν_4 bending modes and that at 385 cm^{-1} relates to ν_2 bending. The very broad weak band from ~3600 to 2800 cm^{-1} corresponds to OH stretching.

Composition

Analyses (3 points) were performed at the University of Utah on a Cameca SX–50 electron microprobe with four wavelength dispersive spectrometers and using *Probe for EPMA* software. Analytical conditions were 15 kV accelerating voltage, 20 nA beam current and a nominal beam diameter of 10 μm. Counting times for each element were 20 s on peak and 10 s each on low and high background. No other elements were detected by energy dispersive spectroscopy. Raw X-ray intensities were corrected for matrix effects with a phi-rho-z algorithm (Pouchou and Pichoir, 1991). Alumolukrahnite exhibits no damage in the electron beam; however, a somewhat rough surface is apparently responsible for the low totals. Because insufficient material was available for a direct determination of H_2O, the amount of water in alumolukrahnite was calculated on the basis of Ca + Cu + Al + Fe + Zn + As = 5 and O = 10 atoms per formula unit, as indicated by the obvious relationship of the mineral to gartrellite, lukrahnite and other members of the tsumcorite group (see below). Analytical data are given in Table 1.

The empirical formula based on 10 O atoms per formula unit is $Ca_{1.01}(Cu_{0.92}Zn_{0.13})_{\Sigma1.05}(Al_{0.96}Fe_{0.01})_{\Sigma0.97}(As_{0.985}O_4)_2(OH)_{0.88}(H_2O)_{1.12}$. The simplified structural formula is $Ca(Cu^{2+},Zn)(Al,Fe^{3+})(AsO_4)_2(H_2O,OH)_2$ and the idealised formula is $CaCu^{2+}Al(AsO_4)_2(OH)(H_2O)$ which requires CaO 12.65, CuO 17.94, Al_2O_3, 11.50, As_2O_5 51.83, H_2O 6.09, total 100 wt.%.

X-ray crystallography

The small size, poor quality and intergrown nature of alumolukrahnite crystals made X-ray single-crystal diffraction study
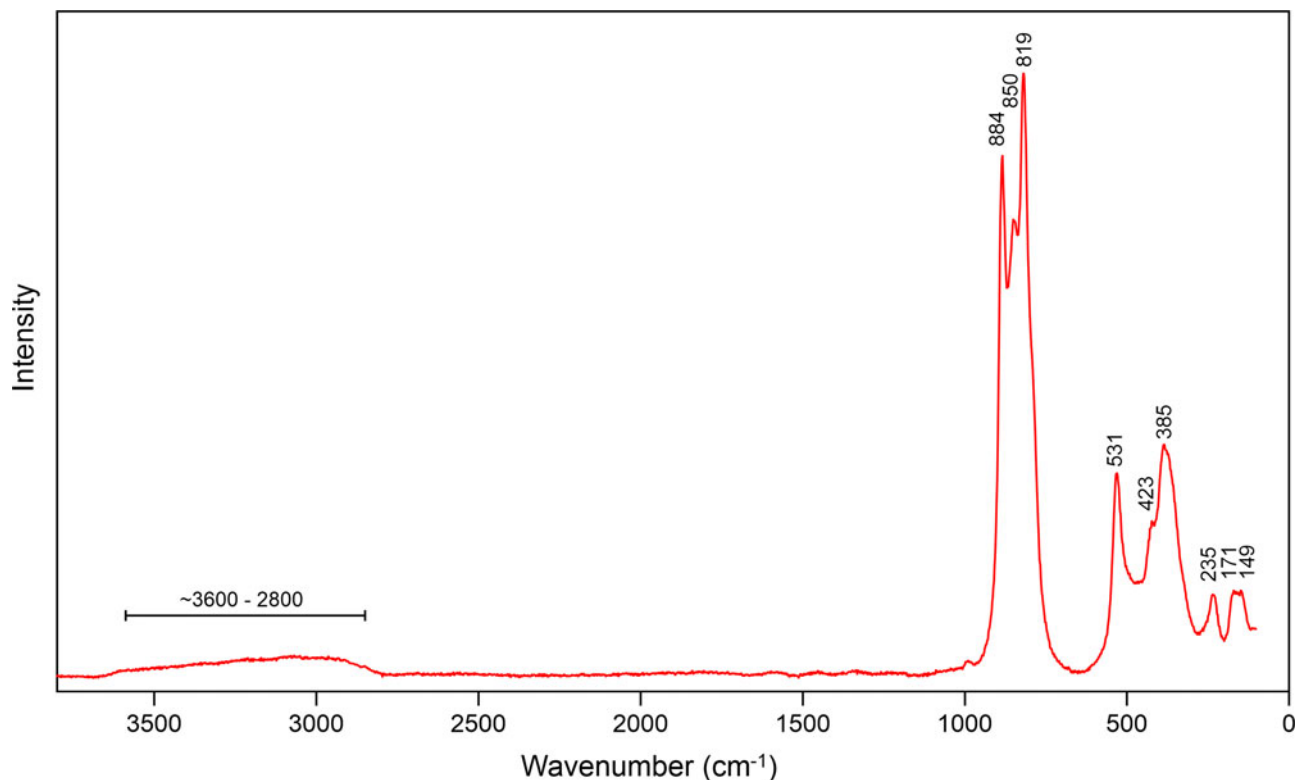

Fig. 1. Alumolukrahnite balls with gypsum (colourless) and coronadite (black) on scorodite (FOV 3.35 mm); specimen #76256.

Fig. 3. Raman spectrum of alumolukrahnite recorded with a 532 nm laser.

Table 1. Analytical data for alumolukrahnite.

Constituent	Mean	Range	S.D.	Standard	Norm.
CaO	12.20	12.10–12.26	0.06	diopside	12.80
CuO	15.62	15.01–15.99	0.38	Cu metal	16.38
ZnO	2.25	2.00–2.46	0.18	Zn metal	2.37
Al_2O_3	10.48	10.14–10.75	0.24	sanidine	10.99
Fe_2O_3	0.22	0.18–0.27	0.03	hematite	0.23
As_2O_5	48.52	48.27–48.78	0.17	syn. GaAs	50.90
H_2O^*	6.03				6.33
Total	95.32				100.00

S.D. – standard deviation; * calculated based on the structure.

impossible. Powder X-ray diffraction (PXRD) data were recorded using a Rigaku R-Axis Rapid II curved imaging plate micro-diffractometer with monochromatised Mo$K\alpha$ radiation. A Gandolfi-like motion on the φ and ω axes was used to randomise the sample. Observed d values and intensities were derived by profile fitting using *JADE Pro* software (Materials Data, Inc.). The unit-cell parameters, refined using whole pattern fitting in *JADE Pro* based on the structure of gartrellite (Krause *et al.*, 1998) with Ca in place of Pb and Al in place of Fe, are space group $P\bar{1}$, $a = 5.343(5)$, $b = 5.501(5)$, $c = 7.329(5)$ Å, $\alpha = 67.72(2)$, $\beta = 69.06(2)$, $\gamma = 69.42(2)°$, $V = 180.3(3)$ Å^3 and $Z = 1$. The
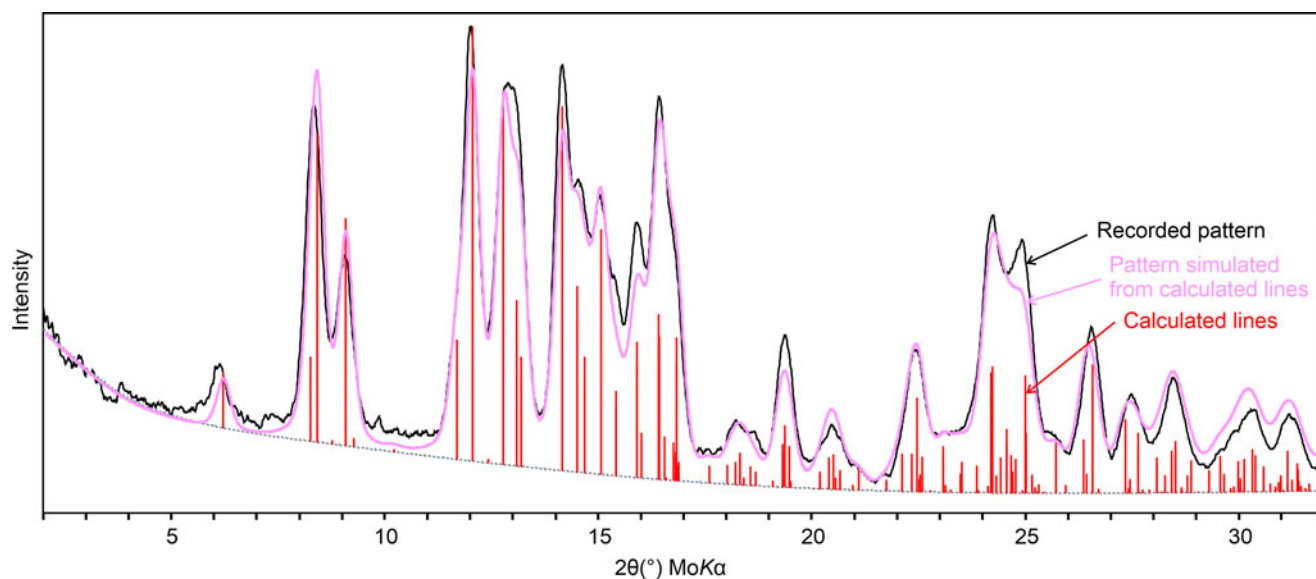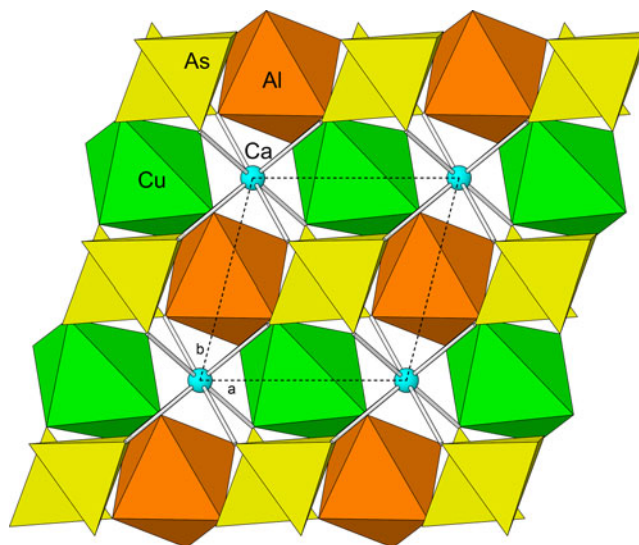

Fig. 4. Powder X-ray diffraction pattern for alumolukrahnite compared with the lines and simulated pattern based on the structure of gartrellite with Ca in place of Pb and Al in place of Fe and with the cell parameters refined using whole pattern fitting.

Table 2. Powder X-ray data (in Å) for alumolukrahnite.

I_{obs}	d_{obs}	d_{calc}	I_{calc}	hkl	I_{obs}	d_{obs}	d_{calc}	I_{calc}	hkl
16	6.66	6.5506	13	0 0 1	9	1.7799	1.7728	11	2 $\bar{1}$ 2
86	**4.89**	4.9284	20	0 1 0	8	1.7520	1.7426	4	1 2 4
		4.8319	71	1 0 0			1.7409	7	$\bar{2}$ 0 2
45	4.50	4.4819	52	1 0 1	13	1.7219	1.7151	6	0 3 1
14	3.504	3.4829	28	0 $\bar{1}$ 1	**65**	**1.6945**	1.6917	28	1 3 3
100	3.396	3.3786	100	1 1 2			1.6893	29	2 2 4
70	3.196	3.1869	86	0 1 2			1.6839	4	2 3 1
70	3.115	3.1107	38	1 0 2	38	1.6649	1.6761	8	0 3 2
		3.0863	25	$\bar{1}$ 1 0			1.6673	15	3 0 1
90	2.882	2.8791	84	$\bar{1}$ $\bar{1}$ 1			1.6607	9	3 2 1
51	2.795	2.8096	43	$\bar{1}$ 1 1			1.6581	5	3 1 0
		2.7746	27	1 $\bar{1}$ 1	52	1.6415	1.6531	8	2 3 3
52	2.714	2.7059	56	1 2 1			1.6387	27	3 1 3
27	2.651	2.6429	20	2 1 1			1.6377	14	0 0 4
51	2.569	2.5644	31	0 2 1			1.6283	4	$\bar{2}$ 1 2
		2.5465	11	1 2 2	11	1.5978	1.5934	12	0 2 4
82	2.488	2.4851	38	2 0 1	44	1.5480	1.5554	12	2 0 4
		2.4814	33	2 1 2			1.5505	5	2 3 0
		2.4642	10	0 2 0			1.5431	30	$\bar{2}$ 2 0
39	2.434	2.4343	9	$\bar{1}$ 0 2	19	1.4995	1.5008	17	1 $\bar{3}$ 1
		2.4267	7	1 1 3			1.4945	3	0 $\bar{3}$ 1
		2.4231	33	0 $\bar{1}$ 2	10	1.4855	1.4841	14	$\bar{3}$ $\bar{1}$ 1
		2.4216	4	2 1 0	8	1.4598	1.4617	8	3 3 3
		2.4159	5	2 0 0			1.4524	4	1 1 5
3	2.314	2.3184	4	0 2 2	27	1.4431	1.4446	10	$\bar{2}$ 0 3
12	2.247	2.2646	4	$\bar{1}$ 1 2			1.4401	11	0 $\bar{2}$ 3
		2.2409	5	2 0 2			1.4395	12	$\bar{2}$ $\bar{2}$ 2
		2.2282	7	1 $\bar{1}$ 2	5	1.4218	1.4264	4	2 2 5
9	2.198	2.1993	4	2 2 1			1.4221	8	$\bar{1}$ 3 2
		2.1835	3	0 0 3	8	1.3917	1.4024	5	$\bar{2}$ 1 3
38	2.112	2.1133	10	0 $\bar{2}$ 1			1.3895	9	1 2 3
		2.1088	14	$\bar{1}$ $\bar{1}$ 2	13	1.3722	1.3859	4	3 $\bar{1}$ 2
		2.0973	10	$\bar{2}$ 0 1			1.3709	7	$\bar{1}$ $\bar{2}$ 3
6	2.026	2.0223	4	$\bar{2}$ 1 1			1.3685	3	0 1 5
13	1.9933	2.0021	7	$\bar{1}$ 2 0	18	1.3547	1.3644	8	1 $\bar{3}$ 1
		1.9917	8	2 2 0			1.3558	10	$\bar{3}$ 1 1
		1.9873	3	$\bar{1}$ 2 1			1.3530	9	2 4 2
		1.9767	5	2 2 3			1.3451	6	1 4 1
3	1.9487	1.9366	5	0 2 3	19	1.3237	1.3278	4	3 3 0
		1.8800	3	2 0 3			1.3214	9	4 2 2
11	1.8440	1.8490	9	$\bar{2}$ 1 1			1.3167	3	$\bar{3}$ 0 2
31	1.8233	1.8299	9	1 1 4	7	1.3068	1.3120	7	2 4 1
		1.8208	22	$\bar{1}$ 0 3			1.3109	5	3 2 5
		1.8162	3	1 3 2			1.3103	3	4 1 1
		1.8150	4	$\bar{1}$ 2 2					
		1.8113	8	0 $\bar{1}$ 3					

Fig. 5. The structure of alumolukrahnite based on that of gartrellite.

resulting calculated PXRD pattern is an excellent fit for the observed alumolukrahnite PXRD pattern (Fig. 4), confirming that alumolukrahnite is isostructural with gartrellite and other triclinic members of the tsumcorite group. Note that the fit with the PXRD pattern of monoclinic members of the tsumcorite group is not as good. The observed and calculated data are compared in Table 2.

Description of the structure

The structure of tsumcorite-group minerals (Krause et al., 1998) consists of edge-sharing chains of $M2$-centred ($M2$ = Fe, Mn, Cu, Zn, Co, Ni and Al) octahedra that are linked by corner sharing with X-centred tetrahedra (X = As, P, V and S) to form sheets with an eight-coordinated $M1$ ($M1$ = Pb, Ca and Na) site nestled between adjacent sheets with $M1$–O bonds linking the sheets into a framework. The general formula is $MlM2_2(XO_4)_2(OH,H_2O)_2$. When there is no significant ordering of cations in the $M2$ site, the structure is generally monoclinic

Table 3. Comparison of selected characteristics for alumolukrahnite and triclinic Cu-arsenate members of the tsumcorite group.

	Alumolukrahnite	Lukrahnite	Gartrellite	Yancowinnaite
Formula	$CaCu^{2+}Al(AsO_4)_2(OH)(H_2O)$	$CaCu^{2+}Fe^{3+}(AsO_4)_2(OH)(H_2O)$	$PbCu^{2+}Fe^{3+}(AsO_4)_2(OH)(H_2O)$	$PbCu^{2+}Al(AsO_4)_2(OH)(H_2O)$
Symmetry	Triclinic, $P\bar{1}$	Triclinic, $P\bar{1}$	Triclinic, $P\bar{1}$	Triclinic, $P\bar{1}$
Cell parameters	a = 5.343(5) Å	a = 5.457(3) Å	a = 5.460(1) Å	a = 5.444(2) Å
	b = 5.501(5) Å	b = 5.539(4) Å	b = 5.653(1) Å	b = 5.640(2) Å
	c = 7.329(5) Å	c = 7.399(6) Å	c = 7.589(2) Å	c = 7.518(2) Å
	α = 67.72(2)°	α = 68.43(5)°	α = 67.68(1)°	α = 67.89(2)°
	β = 69.06(2)°	β = 68.90(4)°	β = 69.27(1)°	β = 69.48(2)°
	γ = 69.42(2)°	γ = 69.44(5)°	γ = 70.04(1)°	γ = 70.18(2)°
	V = 180.3(3) Å³	V = 187.8(3) Å³	V = 196.8(1) Å³	V = 194.51(7) Å³
Z	1	1	1	1
Density$_{calc}$	4.094 g·cm⁻³	4.18 g·cm⁻³	5.43 g·cm⁻³	5.31 g·cm⁻³
Optics	Biaxial (+)	Biaxial (+)	Biaxial (+)	Biaxial (+)
	α = 1.73(1)	α = 1.83(1)	α = 1.94(1)	α = 1.906(5)
	β = 1.74(1)	β = 1.834(calc)	β = 1.98(calc)	β = n.d.
	γ = 1.76(1)	γ = 1.89(2)	γ = 2.06(2)	γ = 1.963(5)
	$2V_{calc}$ = 71°	$2V_{meas}$ = 30(5)°	$2V_{meas}$ = 78(4)°	2V = n.d.
References	This study	Krause et al. (2001)	Krause et al. (1998)	Elliott and Pring (2015)

(although ordering of hydrogen bonds in species with two H_2O per formula unit leads to triclinic symmetry). When the $M2$ site is split with different cations occupying each of the split sites, the structure is triclinic. In all cases of tsumcorite-group $M2$ site splitting, Cu^{2+} occupies one of the split sites, where it assumes 4+2 coordination due to the Jahn–Teller effect. It is also worth noting that, in general, for structures containing essential Cu^{2+} and Al (e.g. ceruleite; Mills *et al.*, 2018), these cations are almost invariably ordered into separate sites because of the different coordination preferences for Cu^{2+} and Al^{3+}. The composition of alumolukrahnite clearly suggests the likelihood of Cu^{2+} and Al ordering at $M2$ and the excellent fit of the PXRD pattern with that calculated based on the triclinic structure supports that conclusion (see above and Fig. 4). The structure of lukrahnite based on that of gartrellite is shown in Fig. 5.

In addition to being the Al analogue of lukrahnite, $CaCuFe^{3+}$ $(AsO_4)_2(OH){\cdot}H_2O$ (Krause *et al.*, 2001) and the Ca–Al analogue of gartrellite, $PbCuFe^{3+}(AsO_4)_2(OH){\cdot}H_2O$ (Nickel *et al.*, 1989; Krause *et al.*, 1998), alumolukrahnite is the Ca analogue of yancowinnaite, $PbCuAl(AsO_4)_2(OH){\cdot}H_2O$ (Elliott and Pring, 2015). Selected characteristics of these minerals are compared in Table 3.

References

Donnay J.H. and Harker D. (1937) A new law of crystal morphology extending the law of Bravais. *American Mineralogist*, **22**, 446–467.

Elliott P. and Pring A. (2015) Yancowinnaite, a new mineral from the Kintore Opencut, Broken Hill, New South Wales. *Australian Journal of Mineralogy*, **17**, 73–76.

Frost R.L., Xi Y. and Palmer S.J. (2012) Raman spectroscopy of the multianion mineral gartrellite-$PbCu(Fe^{3+},Cu)(AsO_4)_2(OH,H_2O)_2$. *Spectrochimica Acta Part A: Molecular and Biomolecular Spectroscopy*, **89**, 93–98.

Kampf A.R., Mills S.J., Housley R.M., Rossman G.R., Nash B.P., Dini M. and Jenkins R.A. (2013) Joteite, $Ca_2CuAl[AsO_4][AsO_3(OH)]_2(OH)_2(H_2O)_5$, a new arsenate with a sheet structure and unconnected acid arsenate groups. *Mineralogical Magazine*, **77**, 2811–2823.

Kampf A.R., Mills S.J., Nash B.P., Dini M. and Molina Donoso A.A. (2015) Tapiaite, $Ca_5Al_2(AsO_4)_4(OH)_4{\cdot}12H_2O$, a new mineral from the Jote mine, Tierra Amarilla, Chile. *Mineralogical Magazine*, **79**, 345–354.

Kampf A.R., Mills S.J., Nash B., Dini M. and Molina Donoso A.A. (2023) Alumolukrahnite, IMA 2022-059. CNMNC Newsletter 70. *Mineralogical Magazine*, **87**, https://doi.org/10.1180/mgm.2022.135

Krause W., Belendorff K., Bernhardt H.-J., McCammon C., Effenberger H. and Mikenda W. (1998) Crystal chemistry of the tsumcorite-group minerals. New data on ferrilotharmeyerite, tsumcorite, thometzekite, mounanaite, helmutwinklerite, and a redefinition of gartrellite. *European Journal of Mineralogy*, **10**, 179–206.

Krause W., Blass G., Bernhardt H.-J. and Effenberger H. (2001) Lukrahnite, $CaCuFe^{3+}(AsO_4)_2[(H_2O)(OH)]$, the calcium analogue of gartrellite. *Neues Jahrbuch für Mineralogie, Monatshefte*, **2001**, 481–492.

Mandarino J.A. (2007) The Gladstone–Dale compatibility of minerals and its use in selecting mineral species for further study. *The Canadian Mineralogist*, **45**, 1307–1324.

Mills S.J., Christy A.G. and Favreau G. (2018) The crystal structure of ceruleite, $CuAl_4$ $[AsO_4]_2(OH)_8(H_2O)_4$, from Cap Garonne, France. *Mineralogical Magazine*, **82**, 181–187.

Nickel E.H., Robinson B.W., Fitz Gerald O. and Birch W.D. (1989) Gartrellite, a new secondary arsenate mineral from Ashburton Downs, W.A. and Broken Hill, N.S.W. *Australian Mineralogist*, **4**, 83–89.

Parker R.L., Salas R.O. and Perez G.R. (1963) Geologia de los distritos mineros Checo de Cobre Pampa Larga y Cabeza de Vaca. *Instituto de Investigaciones Geologicas*, **14**, 40–42.

Pouchou J.-L. and Pichoir F. (1991) Quantitative analysis of homogeneous or stratified microvolumes applying the model "PAP". Pp. 3l–75 in: *Electron Probe Quantitation* (Heinrich, K.F.J. and Newbury, D.E., editors). Plenum Press, New York.

Yang H., Jenkins R.A., Downs R.T., Evans S.H. and Tait K.T. (2011) Rruffite, $Ca_2Cu(AsO_4)_2{\cdot}2H_2O$, a new member of the roselite group, from Tierra Amarilla, Chile. *The Canadian Mineralogist*, **49**, 877–884.